Journal of the Mechanics and Physics of Solids 60 (2012) 1137–1144

Contents lists available at SciVerse ScienceDirect

Journal of the Mechanics and Physics of Solids

journal homepage: www.elsevier.com/locate/jmps

Solitary waves on tensegrity lattices

F. Fraternali [a,*], L. Senatore [a], C. Daraio [b]

[a] Department of Civil Engineering, University of Salerno, 84084 Fisciano (SA), Italy
[b] Engineering and Applied Sciences, California Institute of Technology, Pasadena, CA 91125, USA

ARTICLE INFO

Article history:
Received 26 September 2011
Received in revised form
27 December 2011
Accepted 19 February 2012
Available online 3 March 2012

Keywords:
Tensegrity structures
Solitary waves
Wave profile
Supersonic regime
Atomic-scale localization

ABSTRACT

We study the dynamics of lattices formed by masses connected through tensegrity prisms. By employing analytic and numerical arguments, we show that such structures support two limit dynamic regimes controlled by the prisms' properties: (i) in the low-energy (sonic) regime the system supports the formation and propagation of solitary waves which exhibit $sech^2$ shape and (ii) in the high-energy (ultrasonic) regime the system supports atomic-scale localization. Such peculiar features found in periodic arrays of tensegrity structures suggest their use for the creation of new composite materials (here called "tensegrity materials") of potential interest for applications in impact absorption, energy localization and in new acoustic devices.

1. Introduction

Tensegrity structures attract the interest of researchers working in many different areas, including engineering, mathematics, architecture, biology, and have also inspired beautiful sculptures and artworks (Lalvani, 1996). Such structures consist of spatial assemblies of rigid compressive members (bars) and deformable (prestressed) tensile elements (strings or cables), which typically feature geometrically nonlinear mechanical behavior. Tensegrity networks have been employed as model systems in a large variety of form-finding and dynamical control problems of engineering and architecture (refer, e.g., to You and Pellegrino, 1996; Skelton and Sultan, 2003; Tilbert and Pellegrino, 2003; Motro, 2003; Mask et al., 2006; Sterk, 2006; Zhang et al., 2006; Skelton and de Oliveira, 2010, and references therein). It has been shown in Skelton and de Oliveira (2010) that such structures can form minimal mass systems for given loads, through assemblies of repetitive units forming beautiful 'tensegrity fractals'. The mechanical response of tensegrity structures relies on the basic laws of attraction and repulsion between mass particles and can be suitably adjusted by playing with basic variables, such as mass positions, topology of connections, size, material and prestress of tensile members. It has been recognized in recent years that they well describe the mechanics of a number of biological structures, such as cell cytoskeletons (Ingber, 1998; Wang et al., 2001; Canadas et al., 2002; Mofrad and Kamm, 2006), the red blood cell membrane (Vera et al., 2005), spider fibers (Termonia, 1994), the muscle–bone systems (Ekeberg and Pearson, 2005; Harischandra and Ekeberg, 2008), among others. The tensegrity concept has been employed in space antennas and structures; lightweight and deployable structures; and 'smart' (controllable) systems (refer, e.g., to Skelton and de Oliveira, 2010 and references therein). It is worth noting that a tensegrity structure can be designed optimally strong and stiff, through suitable adjustment of the prestress in the tensile members. Each member, on the other hand, can serve as a sensor or actuator, if proper control systems are implemented (Skelton, 2002).

* Corresponding author.
E-mail addresses: f.fraternali@unisa.it (F. Fraternali), lashton.ku@gmail.com (L. Senatore), daraio@caltech.edu (C. Daraio).

0022-5096/$ - see front matter © 2012 Elsevier Ltd. All rights reserved.
doi:10.1016/j.jmps.2012.02.007

In the present work, we examine a novel application of tensegrity structures, exploring their use as networks supporting energy transport through *solitary waves*. We show that the elastic potential of a 'regular minimal tensegrity prism' (Skelton and de Oliveira, 2010) belongs to the class of nonlinear potentials analyzed in Friesecke and Matthies (2002), which characterize lattices supporting solitary waves with profile dependent on the wave speed. We focus our attention on the symmetrical axial loading of such a system, in order to investigate its highly nonlinear dynamic response within a simple and effective one-dimensional framework. We specifically investigate the waveform of compression waves traveling through chains of tensegrity prisms, showing that the profile of these waves localizes on a single lattice spacing (i.e., on a single prism) in the limit of the wave speed tending to infinity. This feature of tensegrity structures has not yet been investigated in the literature, and could pave the way to the use of 'tensegrity lattices' (or 'crystals') as novel materials to control stress propagation and produce energy trapping (cf., e.g., Fraternali et al., 2010a, 2010b; Daraio et al., 2006 and references therein); innovative tendon- and strut-controlled structures for seismic applications (Skelton, 2002); as well as in novel acoustic devices, in order to create acoustic lenses capable of focusing pressure waves in very compact regions in space (Spadoni and Daraio, 2010).

The paper is organized as follows. We retrace in Section 2 the derivation of the elastic potential of a tensegrity prism (Oppenheim and Williams, 2000), highlighting some features of such a potential that are essential for the subsequent wave analysis. We then develop a numerical study about the profiles of waves traveling through an exemplary tensegrity lattice, considering wave velocities ranging from sonic to supersonic values (Section 3). We show in the same section that the tensegrity prism potential matches the regularity conditions introduced in Friesecke and Pego (1999) and Friesecke and Matthies (2002) to prove existence and basic properties of solitary waves in lattices. We end in Section 4 with a summary of the main conclusions of the present work.

2. Elastic potential of an axially loaded tensegrity prism

Let us consider a *regular minimal tensegrity prism* according to the definition provided in Skelton and de Oliveira (2010). Such a structure consists of two parallel equilateral triangles (end faces), three deformable cross-strings (or cables) and three rigid bars (Fig. 1 (left)). We assume that the end faces are rigid, due to the inextensiblity of the terminal strings and/or the presence of stiff disks at the extremities. In addition, we suppose that the prism is loaded by symmetric axial forces about the longitudinal. Under such assumptions, it can be shown that the prism has a single degree of freedom, which may consist of either the relative twist angle ϕ about the longitudinal axis, or the relative axial displacement r between the end faces (Oppenheim and Williams, 2000).

The constitutive equations of a regular minimal tensegrity prism have been derived in Oppenheim and Williams (2000). We retrace their derivation, in order to highlight some peculiar features of the associated elastic potential. Without loss of

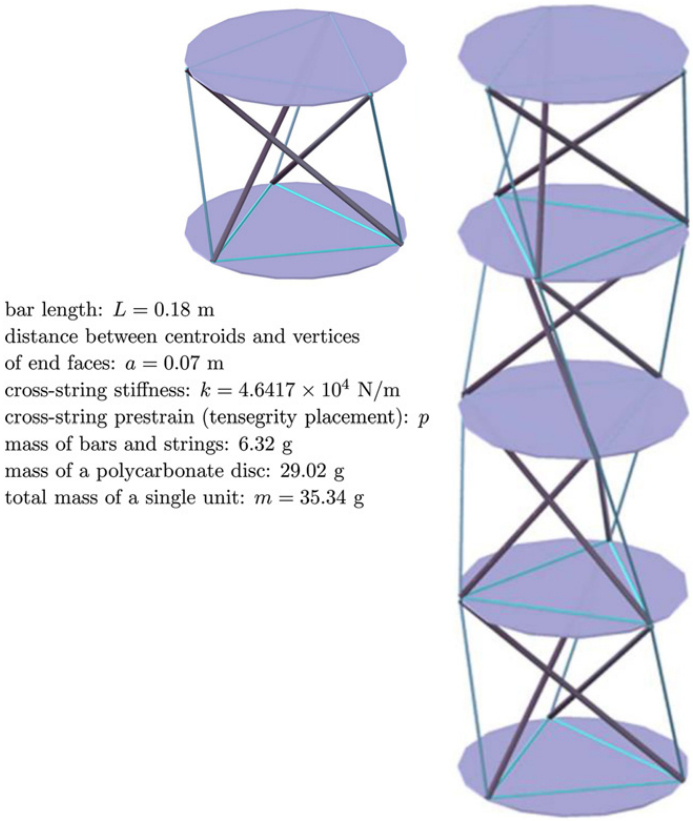

Fig. 1. Illustration of a tensegrity prism (left) and a tensegrity chain (right).

generality, we refer our numerical analysis to the physical model shown in Fig. 1 (left), where the strings are nylon wires of 6 mm diameter; the bars are pultruded carbon tubes (outer diameter: 4 mm; inner diameter: 2.54 mm) with length $L=0.18$ m; the distance a between the centroid and the vertices of the end triangles is equal to 0.07 m; the terminal masses consist of polycarbonate disks with 14 cm diameter and 1.57 mm thickness; and the total mass of a single unit (three bars, three cross-springs, six terminal strings and one polycarbonate disk) is equal to 35.34 g.

On assuming that the end faces are rotated relative to each other by an arbitrary twist angle ϕ, and enforcing the fixed length constraint for the bars, we are led to the following kinematical relationship between ϕ and the prism height h:

$$h=\sqrt{L^2-2a^2(1-\cos\,\phi)} \tag{1}$$

which, once inverted, gives

$$\phi=\arccos\left(1-\frac{L^2-h^2}{2a^2}\right) \tag{2}$$

As shown in Oppenheim and Williams (2000), the lower bound of ϕ is $-\pi/3$ (cross-strings touching each other), while the upper bound of the same quantity is π (legs touching each other). Accordingly, the prism height ranges between the following bounds:

$$h_{lb}=\sqrt{L^2-4a^2},\quad h_{ub}=L \tag{3}$$

with h_{lb} corresponding to $\phi=\pi$, and h_{ub} corresponding to $\phi=0$. It is easily verified (Oppenheim and Williams, 2000) that the cross-string length λ is related to ϕ and h through

$$\lambda=\sqrt{L^2+3a^2\cos\,\phi-\sqrt{3}a^2\sin\,\phi}=\frac{\sqrt{2}}{2}\sqrt{a^2\left(6-\sqrt{3}\sqrt{-\frac{(h^2-L^2)(4a^2+h^2-L^2)}{a^4}}\right)+3\,h^2-L^2} \tag{4}$$

We now compute the elastic potential U of the prism by summing up the potential energies of the cross-strings. Since the latter are given by $k/2(\lambda-\lambda_N)^2$, where k is the stiffness and λ_N is the natural length (length at zero stress) of such elements, we obtain

$$U=\tfrac{3}{2}k(\lambda-\lambda_N)^2 \tag{5}$$

The substitution of (4) onto the right-hand side of (5) leads us to the law relating U with h (or ϕ), which is clearly strongly nonlinear. The axial force F vs h relationship is then obtained as

$$F=\frac{dU}{dh}=3k(\lambda-\lambda_N)\frac{d\lambda}{dh} \tag{6}$$

where

$$\frac{d\lambda}{dh}=\frac{h}{2\lambda}\left(3+\frac{\sqrt{3}(2a^2+h^2-L^2)}{a^2\sqrt{-\frac{(h^2-L^2)(4a^2+h^2-L^2)}{a^4}}}\right) \tag{7}$$

The equilibrium configurations of the prism correspond to $F=0$ and it is possible to show that the unique minimum of U is achieved for $\phi=\phi_0=5/6\pi$ (150^o), within the feasible range of ϕ, assuming that the strings are in tension (such a stable equilibrium configuration will be hereafter referred to as *tensegrity placement*, cf. Oppenheim and Williams, 2000). The twist angle $5/6\pi$ corresponds with the following equilibrium values of the height and cross-string length:

$$h_0=\sqrt{L^2-(2+\sqrt{3})a^2},\quad \lambda_0=\sqrt{L^2-2\sqrt{3}a^2} \tag{8}$$

respectively. The prestrain p of the cross-strings at the tensegrity placement is given by

$$p=\frac{\lambda_0-\lambda_N}{\lambda_N} \tag{9}$$

and is assumed to be positive, as we already noticed. Setting up the tensegrity placement as reference, we define the relative axial displacement r between the end faces as follows:

$$r=h-h_0 \tag{10}$$

with $r\in(r_{lb},r_{ub})$, where $r_{lb}=h_{lb}-h_0<0$, and $r_{ub}=h_{ub}-h_0>0$. We also introduce the following axial strain:

$$\varepsilon=\frac{h_0-h}{h_0} \tag{11}$$

which is positive when the prism is shortened with respect to the tensegrity placement ($r<0$). We refer to the upper bound of ε, i.e. the quantity

$$\varepsilon_{lim}=\frac{h_0-h_{lb}}{h_0} \tag{12}$$

as the *limit strain* of the prism.

The laws relating U and F with r and ε are obtained by making use of (10) and (11) into (5) and (6), respectively. For what concerns the U vs r law, we in particular obtain

$$U(r)=\frac{3}{2}k\left[\frac{\sqrt{3(h_0+r)^2-L^2+a^2(6-\sqrt{3}c(r))}}{\sqrt{2}}-\frac{\lambda_0}{1+p}\right]^2 \tag{13}$$

where

$$c(r)=\sqrt{\frac{[L^2-(h_0+r)^2][4a^2+(h_0+r)^2-L^2]}{a^4}} \tag{14}$$

It is not difficult to realize that the U vs h,r,ε and F vs h,r,ε relationships show vertical asymptotes for $h=h_{lb}$,$r=r_{lb}$ and $\varepsilon=\varepsilon_{lim}$, respectively. Such a 'locking' behavior in compression is characteristic of lattices supporting solitary waves featuring atomic-scale localization in the high-energy limit (Friesecke and Matthies, 2002). The locking behavior is typical, e.g., of Lennard–Jones potentials, which exhibit a minimum point at a given equilibrium distance $d>0$ and blow-up as the distance between neighbor masses tends to zero. It is easily recognized that the locking displacement d of the tensegrity prism (measured from the tensegrity placement) is equal to $-r_{lb}$.

Fig. 2 illustrates the locking behavior of the tensegrity potential

$$V(r)=U(r)-U_0 \tag{15}$$

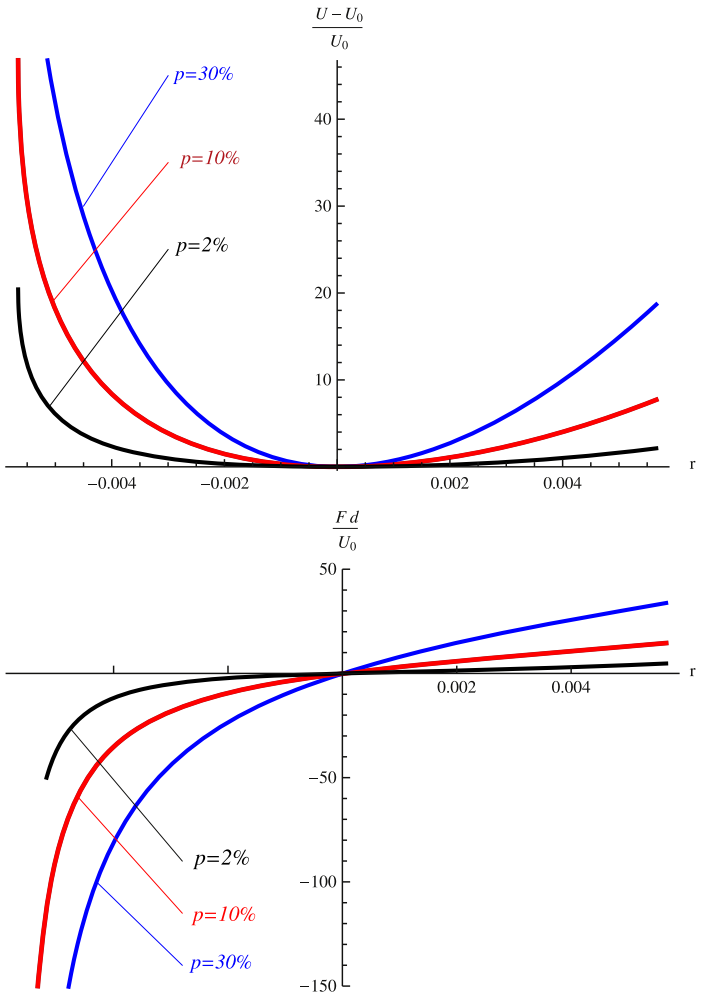

Fig. 2. Normalized V vs r (top) and F vs r (bottom) relationships characterizing the tensegrity prism shown in Fig. 1 (left), for different values of the cross-string prestrain p.

which characterizes the prism shown in Fig. 1 (left), for different values of the cross-string prestrain p ($d=5.66\times10^{-3}$ m; $\varepsilon_{lim}=4.77\%$). Here, U_0 denotes the potential energy of the tensegrity placement, which is not zero due to the prestress of the tensile members.

3. Analysis of solitary waves traveling on tensegrity chains

It has been shown in Friesecke and Pego (1999) and Friesecke and Matthies (2002) that one-dimensional lattices endowed with suitable nonlinear interaction potentials (like, e.g., Lennard–Jones potentials of the form $V_{LJ}(r)=c((r+d)^{-m}-d^{-m})^2$, cf. Friesecke and Matthies, 2002) are traversed by solitary waves with profile dependent on the ratio between the wave speed c and the sound speed c_s. In particular, the potentials examined in Friesecke and Matthies (2002) support atomic-scale localization of solitary waves in the high-energy limit, and feature the following regularity conditions:

- (H1) *minimum at zero*: $V\in C^3(-d,\infty), V\geq 0, V(0)=0, V''(0)>0$;
- (H2) *growth*: $V(r)\geq c_0(r+d)^{-1}$, for some $c_0>0$ and all r close to $-d$;
- (H3) *hardening*: $V'''(r)<0$ in $(-d,0]$, $V(r)<V(-r)$ in $(0,d)$.

For $c\approx c_s$, the continuum limits of the strain waves traveling on lattices endowed with such potentials have a small-amplitude profile of the form $\varepsilon_c(x)=\varepsilon_{sech^2}(x)+O(\gamma^4)$ (Friesecke and Pego, 1999), where x is a coordinate centered at the wave peak, and it results

$$\varepsilon_{sech^2}(x)=-\frac{a}{bh_0}\left(\frac{\gamma}{2}\,\mathrm{sech}\left(\frac{\gamma x}{2h_0}\right)\right)^2 \tag{16}$$

with

$$\gamma^2=24\frac{c-c_s}{c_s},\quad a=V''(0),\quad b=V'''(0) \tag{17}$$

$$c_s=h_0\sqrt{\frac{V''(0)}{m}} \tag{18}$$

h_0 denoting the lattice spacing. Differently, for $c\gg c_s$ (that is, $c\to\infty$), the strain waves tend to assume a piecewise linear profile $\varepsilon_\infty(x)$, which is concentrated on a single lattice spacing and defined as follows (Friesecke and Matthies, 2002):

$$\varepsilon_\infty(x)=\begin{cases}0 & \text{if } x/h_0\leq -1\\ d/h_0\ (1-|x/h_0|) & \text{if } x/h_0\in[-1,1]\\ 0 & \text{if } x/h_0\geq 1\end{cases} \tag{19}$$

It is not difficult to show that the tensegrity potential (15) matches the above conditions (H1) and (H2). In particular, the condition of minimum at zero (H1) is a consequence of our choice of the tensegrity placement as reference, while the growth condition (H2) follows from the vertical asymptote of the tensegrity potential $V(r)$ at $r=r_{lb}=-d$ (Fig. 2). Concerning the hardening condition (H3), (Friesecke and Matthies, 2002) observe that such a property is verified if it results in $V'''(r)<0$ in $(-d,d]$. Numerical computations show that the latter condition is matched by the tensegrity potentials analyzed in the present study.

We numerically investigate the dynamics of chains of 300 tensegrity prisms featuring the properties shown in Fig. 1 ($c_s=147.5$ m/s), by analyzing the strain waves ε_{tens} that are produced by the impact of an external striker of mass $m_s=28$ g with the chain. We numerically determine the speed, amplitude and profile of ε_{tens} at the steady state, employing a

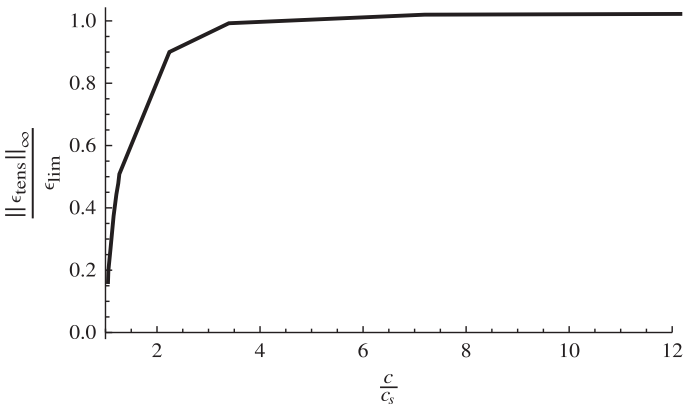

Fig. 3. Ratio between the L^∞ norm of the strain wave amplitude in tensegrity chains ($\|\varepsilon_{tens}\|_\infty$) and the limit strain ε_{lim}, as a function of the ratio between the wave speed c and the sound speed c_s.

fourth-order Runge–Kutta integration scheme (Fraternali et al., 2010b) to solve the Newton equations of motion of the different masses forming the system. The chain is described as a mass-spring system, by lumping the prisms' masses (largely due to the terminal polycarbonate disks, cf. Fig. 1) at the end faces, and modeling the prisms as nonlinear elastic springs governed by potential (15). We consider a prestrain $p=2\%$ of the cross-strings, and adopt a time-integration step equal to 10^{-8} s. We generate waves with different speeds by prescribing different impact velocities to the striker.

Fig. 3 shows the numerical correlation that we obtain between the L^∞ norm ($\|\varepsilon_{tens}\|_\infty$) of ε_{tens} (i.e., the *essential supremum* of $|\varepsilon_{tens}|$, refer, e.g., to Adams, 1975) and the wave speed c. It is seen that $\|\varepsilon_{tens}\|_\infty$ asymptotically converges to the limit strain ε_{lim} for $c\to\infty$, with $\|\varepsilon_{tens}\|_\infty > 0.99\ \varepsilon_{lim}$ for $c \geq 3.4c_s$.

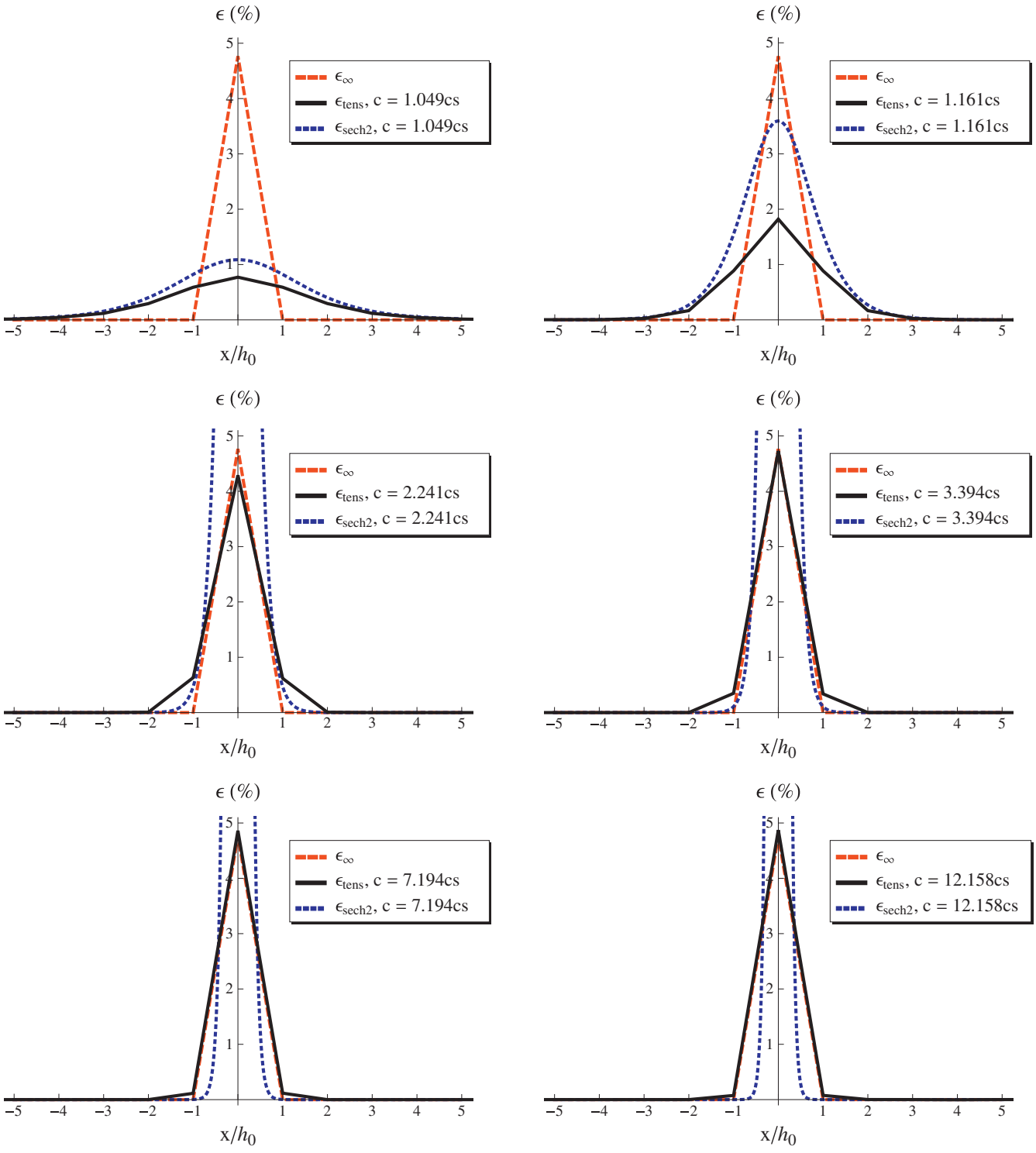

Fig. 4. Strain wave profiles in tensegrity chains (ε_{tens}; black solid lines) for different wave speeds, in comparison with theoretical sonic (ε_{sech^2}; blue dotted lines) and supersonic (ε_∞; red dashed lines) profiles. (For interpretation of the references to color in this figure legend, the reader is referred to the web version of this article.)

The profiles $\varepsilon_{tens}(x)$ corresponding to different wave speeds c are illustrated in Fig. 4. Such a figure highlights that the ε_{sech^2} profile (16) always features an amplitude larger than ε_{tens}, over the entire window $c \in [1.05,\ 12.16]c_s$. In particular, we observe a good match between ε_{sech^2} and ε_{tens} for $c = 1.05c_s$, and, on the contrary, marked deviations between such profiles for $c \geq 1.16c_s$. The results in Fig. 4 also reveal that $\varepsilon_{tens}(x)$ is localized on about seven prisms for $c = 1.05c_s$; five prisms for $c = 1.16c_s$; and three prisms for $c = 2.24c_s$ and $c = 3.39c_s$. When $c = 7.19c_s$ and $c = 12.16c_s$, we instead observe that the values of $\varepsilon_{tens}(x)$ at $x = \pm h_0$ are negligible compared to $\varepsilon_{tens}(0)$, which implies the localization of ε_{tens} on a single prism. In particular, $\varepsilon_{tens}(x)$ practically coincides with the supersonic profile (19) for $c = 12.16c_s$.

4. Concluding remarks

We have discussed a novel application of tensegrity structures as devices supporting energy transport through solitary waves. We have proved that the elastic potential of a regular minimal tensegrity prism subject to symmetric axial loading (Oppenheim and Williams, 2000) matches the regularity conditions required by the analysis presented in Friesecke and Pego (1999) and Friesecke and Matthies (2002) to prove the existence of solitary waves on lattices. We have also numerically shown that solitary waves traveling through a model tensegrity lattice approximatively span blocks of 5–7 prisms, when the wave speed c is almost equal to the speed of sound c_s. In the same ('sonic') regime, the wave profile approximatively exhibits a sech^2 shape. The wave width progressively shrinks for increasing values of c, leading to a piecewise linear wave profile featuring 'atomic-scale localization' of the wave (that is, localization on a single prism) for $c \to \infty$. The above features of tensegrity lattices can be suitably tuned by playing with mass, stiffness, prestress and geometrical properties, with the aim of performing desired wave localization for prescribed wave speed ranges. Such systems could be usefully exploited to design innovative 'tensegrity crystals' suitable for application in stress mitigation and redirection; controllable structures for seismic applications; as well as in acoustic systems and devices. In future work, we intend to explore the dynamics of tensegrity lattices under asymmetric loading, as well as the 3D dynamic response of tensegrity networks of arbitrary shape.

Acknowledgments

The authors greatly acknowledge the support and advice received by Robert Skelton. F.F. and L.S. also thank the Graduate Aerospace Laboratory at the California Institute of Technology (GALCIT) for the hospitality during their visits. C.D. acknowledges the Office of Naval Research (YIP), and the US National Science Foundation grant number 844540 (CAREER). FF acknowledges the support of the Italian Network of Seismic Engineering Laboratories (ReLUIS) and the Italian Civil Protection Department (DPC), through the ReLUIS-DPC grant 2010/2013.

References

Adams, R., 1975. Sobolev Spaces. Academic Press.
Canadas, P., Laurent, V.M., Oddou, C., Isnbey, D., Wendling, S., 2002. A cellular tensegrity model to analyse the structural viscoelasticity of the cytoskeleton. J. Theor. Biol. 218, 115–173.
Daraio, C., Nesterenko, V.F., Herbold, E., Jin, S., 2006. Energy trapping and shock disintegration in a composite granular medium. Phys. Rev. Lett. 96. 058002-1–4.
Ekeberg, O., Pearson, K., 2005. Computer simulation of stepping in the hind legs of the cat: an examination of mechanisms regulating the stance-to-swing transition. J. Neurophysiol. 94 (6), 4256–4268.
Fraternali, F., Blesgen, T., Amendola, A., Daraio, C., 2010a. Multiscale mass-spring models of carbon nanotube foams. J. Mech. Phys. Solid. 59 (1), 89–102.
Fraternali, F., Porter, M., Daraio, C., 2010b. Optimal design of composite granular protectors. Mech. Adv. Mat. Struct. 17, 1–19.
Friesecke, G., Matthies, K., 2002. Atomic-scale localization of high-energy solitary waves on lattices. Physica D 171, 211–220.
Friesecke, G., Pego, R., 1999. Solitary waves on FPU lattices: I. Qualitative properties, renormalization and continuum limit. Nonlinearity 12, 1601–1627.
Harischandra, N., Ekeberg, O., 2008. System identification of muscle–joint interactions of the cat hind limb during locomotion. Biol. Cybern. 99 (2), 125–138.
Ingber, D., 1998. The architecture of life. Sci. Am., 48–57.
Lalvani, H., 1996. Origins of tensegrity: views of Emmerich, Fuller and Snelson. Int. J. Space Struct. 11, 27–55.
Mask, M., Skelton, R.E., Gill, P.E., 2006. Optimization of tensegrity structures. Int. J. Solids Struct. 43 (16), 4687–4703.
Mofrad, M.R.K., Kamm, R.D., 2006. Introduction, with the biological basis for cell mechanics. In: Mofrad, M.R.K., Kamm, R.D. (Eds.), Cytoskeletal Mechanics: Models and Measurements, Cambridge University Press, pp. 1–17.
Motro, R., 2003. Tensegrity: Structural Systems for the Future. Kogan Page Science, London.
Oppenheim, I., Williams, W., 2000. Geometric effects in an elastic tensegrity structure. J. Elast. 59, 51–65.
Skelton, R.E., 2002. Structural systems: a marriage of structural engineering and system science. J. Struct. Control 9, 113–133.
Skelton, R.E., de Oliveira, M.C., 2010. Tensegrity Systems. Springer.
Skelton, R.E., Sultan, C., 2003. Deployment of tensegrity structures. Int. J. Solids Struct. 40, 4637–4657.
Spadoni, A., Daraio, C., 2010. Generation and control of sound bullets with a nonlinear acoustic lens. Proc. Natl. Acad. Sci. 107. 7230–1–5.
Sterk, T., 2006. Shape control in responsive architectural structures—current reasons and challenges. In: Proceedings of the Fourth World Conference on Structural Control and Monitoring, San Diego, CA, USA.
Termonia, Y., 1994. Molecular modeling of spider silk elasticity. Macromolecules 27, 7378–7381.
Tilbert, A.G., Pellegrino, S., 2003. Review of form-finding methods for tensegrity structures. Int. J. Space Struct. 18 (4), 209–223.

Vera, C., Skelton, R.E., Bosscns, F., Sung, L.A., 2005. 3-D nanomechanics of an erythrocyte junctional complex in equibiaxial and anisotropic deformations. Ann. Biomed. Eng. 33 (10), 1387–1404.
Wang, N., Naruse, K., Stamenoviá, D., Fredberg, J.J., Mijailovich, S.M., Toliá-Nrrelykke, I.M., Polte, T., Mannix, R., Ingber, D.E., 2001. Mechanical behavior in living cells consistent with the tensegrity model. Proc. Natl. Acad. Sci. 98 (14), 7765–7770.
You, Z., Pellegrino, S., 1996. Cable-stiffened pantographic deployable structures. Part 1: Triangular mast. AIAA J. 34, 813–820.
Zhang, L., Maurin, B., Motro, R., 2006. Form-finding of non-regular tensegrity systems. J. Struct. Eng. 132 (9), 1435–1440.